# Engineering bone tissue from human embryonic stem cells

Darja Marolt[a,1], Iván Marcos Campos[a], Sarindr Bhumiratana[a], Ana Koren[a,b], Petros Petridis[a], Geping Zhang[c], Patrice F. Spitalnik[c], Warren L. Grayson[d], and Gordana Vunjak-Novakovic[a,2]

[a]Department of Biomedical Engineering, and [c]Department of Pathology and Cell Biology, College of Physicians and Surgeons, Columbia University, New York, NY 10032; [b]Blood Transfusion Centre of Slovenia, Ljubljana, SI-1000, Slovenia; and [d]Department of Biomedical Engineering, School of Medicine, The Johns Hopkins University, Baltimore, MD 21231

In extensive bone defects, tissue damage and hypoxia lead to cell death, resulting in slow and incomplete healing. Human embryonic stem cells (hESC) can give rise to all specialized lineages found in healthy bone and are therefore uniquely suited to aid regeneration of damaged bone. We show that the cultivation of hESC-derived mesenchymal progenitors on 3D osteoconductive scaffolds in bioreactors with medium perfusion leads to the formation of large and compact bone constructs. Notably, the implantation of engineered bone in immunodeficient mice for 8 wk resulted in the maintenance and maturation of bone matrix, without the formation of teratomas that is consistently observed when undifferentiated hESCs are implanted, alone or in bone scaffolds. Our study provides a proof of principle that tissue-engineering protocols can be successfully applied to hESC progenitors to grow bone grafts for use in basic and translational studies.

tissue regeneration | pluripotent stem cells

Repair of large bone defects resulting from trauma, congenital malformations, and surgical resections remains a challenge that is being addressed by advanced tissue engineering approaches (1, 2). The requirements for treating large bone defects include derivation of sufficient numbers of therapeutic cells, use of mechanically and structurally competent osteogenic scaffolds, and facilitation of the synergistic development of the bone and vascular supply to maintain graft viability and function and initiate remodeling (3–7).

The "biomimetic" approach to bone tissue engineering involves the cultivation of cells in 3D scaffolds designed to mimic the composition, structure, and biomechanics of the native bone matrix, with medium perfusion designed to provide the necessary hydrodynamic shear. These scaffold-bioreactor systems regulate bone formation by presenting the cells with conditions resembling those encountered during normal development (8). In addition to clinical utility, such tissue models of high biological fidelity could also provide valuable tools for studies of development and disease (9).

In bone, coordinated function of specialized cell types— osteoblasts, osteoclasts, vascular cells, bone marrow populations, and neurons—preserves the proper shape, structure, and integrity of the tissue (10). Pluripotent human embryonic stem cells (hESC) are uniquely suited for engineering of bone, because they can give rise to unlimited numbers of all specialized cells present in the bone (11). Prior work has demonstrated the potential of hESC to differentiate into mesenchymal cells (12–15), osteoblasts (16–18), chondrocytes (19, 20), endothelial cells (21), cardiovascular cells (22), and neurons (23). Several studies indicated that the hESC-derived mesenchymal progenitors could be similar to the adult bone marrow-derived mesenchymal stem cells (BMSC) (13). hESCs represent an invaluable model for studies of human cell differentiation and share many similarities with the induced pluripotent stem cells (iPSC) that can be derived from patients for autologous use (24–26).

The goal of our study was to establish feasibility of engineering fully viable, ~0.5-cm-large compact bone constructs from hESC, and to evaluate their phenotypic stability and safety in a s.c. implantation model. In prior studies, only limited formation of bone tissue was achieved and was accompanied with the development of teratomas containing numerous other cell types (17, 27, 28). As a result, the conditions that selectively support development of bone from hESC, either in vitro or in vivo, remain largely unknown.

We demonstrate that the hESC-derived mesenchymal progenitors can be induced to form compact, homogenous, and phenotypically stable bone-like tissue by cultivation on 3D osteoconductive scaffolds in bioreactors with interstitial flow of culture medium. Notably, engineered bone grafts contained dense bone matrix, further matured over 8 wk of s.c. implantation, supported ingrowth of vasculature, and showed signs of initial remodeling, without a single incidence of teratoma. In striking contrast, s.c. implantation of undifferentiated hESC either in osteoconductive scaffolds or in Matrigel resulted in consistent formation of teratomas. We propose that engineering bone-like tissue from human pluripotent cells can help advance fundamental study of osteogenesis and translation into regenerative medicine applications.

## Results and Discussion

**Bone Tissue Engineering Model System.** We developed a stepwise protocol to engineer bone-like constructs from hESC (Fig. 1). To mimic the progression of bone development, which starts with condensation of mesenchymal cells (29), we induced mesenchymal differentiation of hESC in serum-supplemented medium. Subsequently, hESC-derived progenitors were differentiated into bone by cultivation in osteoconductive scaffolds using perfusion bioreactors with interstitial flow of osteoinductive culture medium (30, 31). Because hESC can differentiate into mixed populations of cells that pose a risk of subsequent tumor formation (17), the phenotypic stability of engineered bone was evaluated in SCID-beige mice.

**Derivation of Mesenchymal Progenitors of hESCs.** Undifferentiated hESCs give rise to cells resembling the mesenchymal stem cells either spontaneously, in coculture with adult cells, or after exposure to differentiation-inducing factors (12–15). We induced the differentiation of two lines of hESC (H9 and H13) in monolayer culture by simply supplementing culture medium with
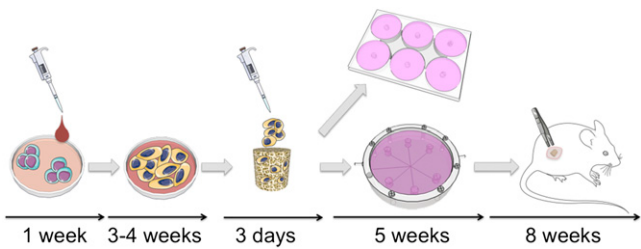
MEDICAL SCIENCES

www.manaraa.com

**Fig. 1.** Bone engineering protocol and timeline. Undifferentiated hESC were cultured in mesoderm-inducing medium for 1 wk. Adherent cells were expanded in monolayer for 4 passages (3–4 wk) and seeded on decellularized bone scaffolds in osteogenic medium for 3 d to allow cell attachment. Cell-seeded constructs were then cultured in osteogenic medium for 5 wk in either perfusion bioreactors or static dishes. Tissue development was evaluated after 3 and 5 wk of culture. Bioreactor-grown bone was implanted s.c. in SCID-beige mice for 8 wk to evaluate tissue stability and maturation.

serum and eliminating bFGF for 7 d, after which the cultures were passaged. Between passages 1 and 3, our protocol resulted in adherent progenitors exhibiting continuous growth (Fig. S1A), fibroblastic morphology (Fig. S1A), and homogenous expression of mesenchymal surface antigens CD44, CD73, CD90, CD105, and CD166 (Fig. S1C). Antigens marking pluripotent stem cells

(SSEA-4), early differentiation (SSEA-1), endothelial- (CD31), hematopoetic- (CD34), and neuroectodermal-mesenchymal (CD271) lineages were not expressed (Fig. S1C).

hESC-derived progenitors exhibited the potential for mesenchymal differentiation in vitro comparable to that of BMSC (Fig. S1B) (32). Strong osteogenic potential of hESC progenitors was evidenced by alkaline phosphatase activity and matrix mineralization in osteogenic medium (Fig. S1B). Both the chondrogenic potential of cells cultured in chondrogenic medium that was evidenced by the presence of Alcian Blue-positive glycosaminoglycan and the adipogenic potential of cells cultured in adipogenic medium that was evidenced by the oil red staining were weaker for hESC progenitors than BMSCs (Fig. S1B). These findings are consistent with previous reports for other hESC lines (18, 33).

**Robust Development of Bone Matrix in Perfused Bioreactor Cultures.**
We reported the formation of bone-like tissues by adult BMSCs cultured for 5 wk on decellularized bone scaffolds (30, 34, 35) and it has been shown that medium perfusion through cell-seeded scaffolds was critical for the viability and maturation of engineered bone (30, 34, 36–38). The flow velocities providing sufficient oxygen to maintain cell viability in large scaffolds ranged from 0.08 to 1.8 mm/s—with 0.8 mm/s being optimal for bone formation, corresponding to the initial fluid shear in the

**Fig. 2.** Effects of bioreactor cultivation on bone tissue development. (A) DNA content per wet weight (ww) of tissue constructs was expressed as percent initial value (at the start of bioreactor/static cultivation) and found to be significantly higher in bioreactor groups (br) compared with the static group (st). (B) Similarly, significantly higher alkaline phosphatase (AP) activity was observed after 3 wk of culture in the H9 bioreactor group. Both DNA content and AP activity increased significantly in the static group from week 3 to week 5. (C) Cumulative osteopontin (OPN) release into culture medium was significantly higher after 2 wk of culture (medium change 4 and later) in the bioreactor groups than in static groups. Data represent averages ± SD (n = 3–5; P < 0.05; * and #, statistically significant differences from the H9 bioreactor and BMSC bioreactor groups at the same timepoint; $, a statistically significant difference within the group between week 3 and week 5). (D) Positive effects of bioreactor culture were corroborated by histological analyses, showing denser tissue deposition in the bioreactor groups compared with the static group after 5 wk of culture (Hematoxylin Eosin; Top). Deposition of bone matrix was confirmed by positive staining of collagen (Masson Trichrome, blue color; Middle Upper), osteocalcin (brown color; Middle Lower), and osteoid (Goldner Trichrome, red color; Bottom). Only minimal staining was observed in statically cultured constructs at weeks 3 and 5. Black T lines mark the position where low magnification micrographs were overlayed. Inset represents negative staining control.
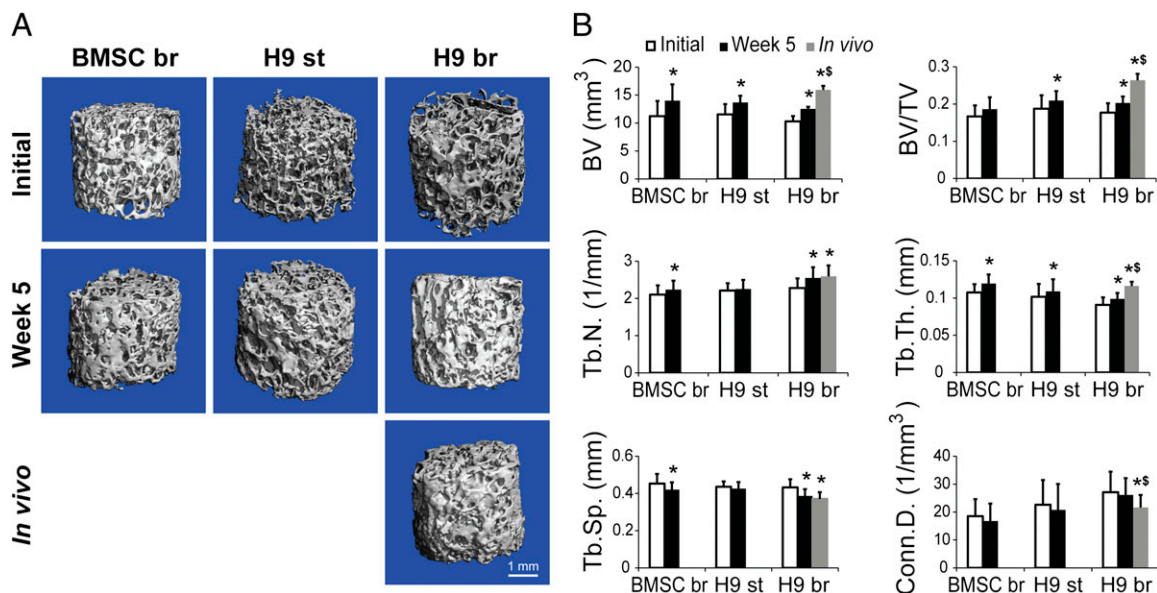
www.manaraa.com
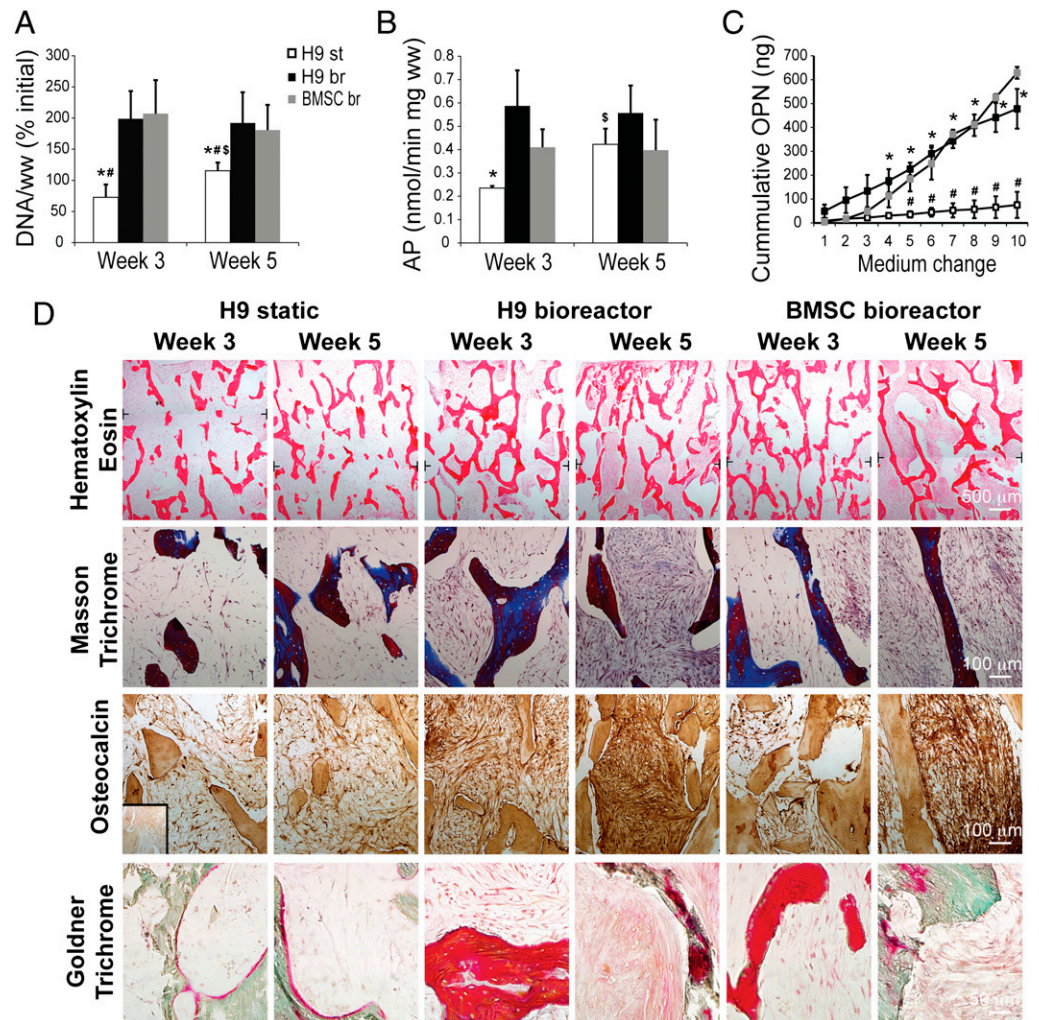
**Fig. 3.** Engineered bone mineralization. (*A*) Reconstructed 3D μCT images of the tissue engineered bone constructs from H9-derived progenitors and BMSCs before cultivation, after 5 wk of cultivation, and after 8 wk of implantation indicated formation of mineralized tissue in all groups. (*B*) Bone structural parameters determined by μCT analysis indicated bone maturation during in vitro culture and in vivo implantation. Bone volume (BV), bone volume fraction (BV/TV), trabecular number (Tb.N.), and trabecular thickness (Tb.Th.) all increased significantly in the H9 bioreactor group, consistent with the decrease in trabecular spacing (Tb.Sp.). Similar changes in mineralized tissue were noted for the H9-static and BMSC-bioreactor groups. Data represent averages ± SD ($n$ = 4; $P$ < 0.05; * and \$, statistically significant differences from initial values and from week 5 values within the same group).

range of 0.6 and 20 mPa, which increased with the deposition of a new bone matrix (30).

Bone tissue engineering protocols established in these studies for adult mesenchymal stem cells were applied in the present study to mesenchymal progenitors derived from hESCs, using the flow velocity of 0.8 mm/s. Our rationale was that the operating conditions shown optimal for BMSC (30) will also support the survival and formation of bone by hESC-derived mesenchymal progenitors. Perfused bioreactor cultures of hESC-progenitors had significantly higher cell numbers (Fig. 2*A* and Fig. S2*A*), alkaline phosphatase activity (Fig. 2*B* and Fig. S2*B*), osteopontin release (Fig. 2*C* and Fig. S2*C*), and bone matrix density (Fig. 2*D* and Fig. S2*D*) than the corresponding static cultures. The effects of perfusion were comparable for constructs grown by using hESC and BMSC (Fig. 2 *A–C*). In comparison with the H9 line, the H13 line exhibited slightly lower cellularity and more variation in tissue density and distribution (Fig. 2 and Fig. S2), suggesting differences in attachment and/or growth pattern between different cell lines. Overall, the acceleration of tissue development in constructs engineered from both hESC and BMSC indicates the vital role of interstitial medium flow in bone formation (Fig. 2 and Fig. S2).

Histological examinations revealed that the matrix produced by hESC-derived progenitors and BMSC contained collagen, osteopontin, bone sialoprotein, and osteocalcin, which indicate the development and maturation of bone specific matrix (Fig. 2*D* and Fig. S3) and the formation of osteoids (Fig. 2*D* and Fig. S3*B*). In contrast to static cultures, which showed only scarce deposition of bone matrix, perfused cultures yielded dense bone matrix (Fig. 2 and Fig. S3), with the density of homogenously distributed bone matrix being comparable for perfused hESC-progenitor and BMSC constructs (Fig. S3). These data suggest that hESC-mesenchymal progenitors continue to mature toward bone-depositing osteoblasts.

The accumulation and maturation of bone-like tissue was confirmed by μCT imaging (Fig. 3 and Fig. S4) that evidenced significant increases in mineralized bone volume and trabecular

thickness, along with significant decreases in trabecular spacing in perfused constructs formed from H9, H13, and BMSC (Fig. 3 and Fig. S4), confirming the progression of mineralization.

Our results demonstrate that tissue engineering parameters determined for BMSC can be translated to hESC-derived mesenchymal progenitors, with implication to engineering of clinical-size grafts (35), composite grafts (39), and testing of novel biomaterials (40). It remains to be determined whether hESC-mesenchymal progenitors derived by different protocols (12, 18) would exhibit similar functional properties.

**Engineered Bone Tissue Remains Stable in Vivo, with Evidence of Maturation, Vascularization, and Remodeling.** To establish safety of hESC-engineered bone constructs, it is critical to evaluate their phenotypic stability in an in vivo setting (17, 27). We selected to test the stability of engineered bone grafts in a s.c. transplantation model in immunodeficient mouse, which is frequently used to assess cells and scaffolds in bone tissue engineering, and for evaluation of pluripotent stem cells (17, 25).

Undifferentiated hESCs implanted either in Matrigel or in osteogenic scaffolds invariably formed teratomas containing lineages of all three germ layers by 7 wk in vivo (Fig. 4*A*). hESC-mesenchymal progenitors implanted on bone scaffolds after 3-d seeding but without further in vitro cultivation exhibited some signs of osteogenesis, shown by formation of loose connective tissue that was weakly positive for bone matrix proteins (Fig. 4 *A* and *B*). The lack of evidence of other germ-layer tissues suggests that our induction protocol is sufficient to restrict the pluripotency of hESCs (confirmed by the presence of teratomas in hESC transplantation groups) to mesenchymal lineages. Similar absence of tumors has been reported in a recent study where hESC-mesenchymal progenitors were injected s.c. into immunodeficient mice for up to 6 mo (41). In another study, where bioreactor cultivation was not used to support in vitro bone maturation, mesenchymal induction resulted in teratomas between 8 and 20 wk in vivo, suggesting that longer studies may be needed to validate the safety of specific differentiation protocols (17). As an
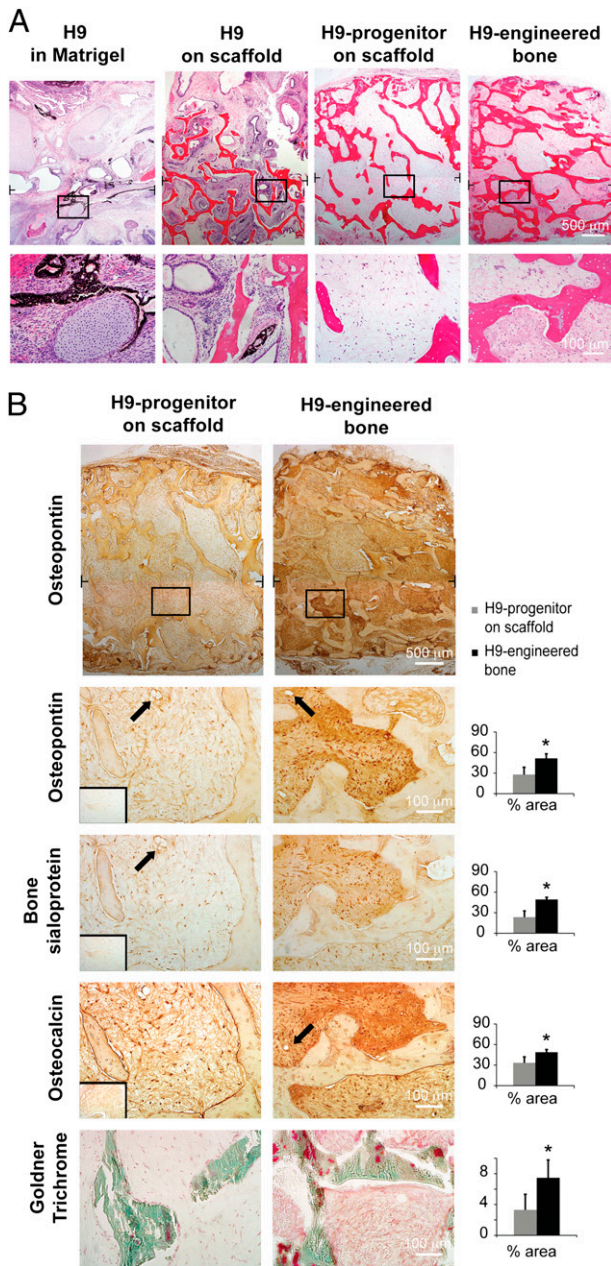
Marolt et al.

MEDICAL SCIENCES

**Fig. 4.** Stability of engineered bone implanted in vivo. Histological analysis indicated stability of mature bone phenotype in H9-engineered bone after 8 wk of s.c. implantation. (*A*) In contrast, a formation of loose connective tissue was detected in bone scaffolds seeded with H9-progenitors before implantation, and teratoma tissue was found in implants formed from undifferentiated H9 cells in either bone scaffolds or Matrigel. Brackets denote positions of high magnification images. (*B*) Quantitative histomorphometric analyses indicated significantly larger fractional area staining positively (brown color) for bone markers osteopontin (*Top* and *Middle Top*), bone sialoprotein (*Middle*) and osteocalcin (*Midle Bottom*), compared with scaffolds seeded with H9-derived progenitors. *Insets* represent negative staining controls. Similarly, significantly higher area fractions covered with osteoids (red color; *Bottom*) were detected in engineered bone compared with scaffolds seeded with H9-derived progenitors. Data represent average ± SD ($n = 5$; $P < 0.01$; *, statistically significant differences between the groups). Arrows mark the presence of microvessels. Black T lines mark the positions where low magnification micrographs were overlayed.

alternative to the extended hESC-mesenchymal induction, cell purification by fluorescent-activated cell sorting for specific mesenchymal markers could be implemented (14).

Notably, engineered bone maintained dense homogenous bone protein matrix over 8 wk in vivo (Fig. 4*B*), with highest-density areas adjacent to the scaffold structure. Cell lineages that are not present in bone were not detected in these constructs. The human origin of the cells was confirmed by nuclear staining (Fig. S5). Bone explants were surrounded by loose connective tissue capsules and contained functional microvasculature containing blood cells in the interior of engineered tissues. We also observed osteoclast invasion at the construct edges, suggesting the initiation of scaffold resorption (Fig. S5).

The μCT examination of the engineered bone explanted after 8 wk in vivo supported continued maturation of engineered bone, with significant increases in bone volume, bone volume to tissue volume ratio, and trabecular thickness compared with the constructs at the time of implantation (after 5 wk of culture; Fig. 3). The total increases in bone volume—an average of 2.2 mm$^3$ during the 5 wk of in vitro culture and an additional 3.4 mm$^3$ during 8 wk in vivo—were within the ranges reported for new bone formation after implantation of growth-factor releasing scaffolds for repair of critically sized bone defects (42).

Together with the presence of osteoclasts invading the constructs in the periphery region, these findings suggest that the combined effects of osteoinductive bone scaffolds and bioreactor cultivation yield engineered constructs with potential for enhanced bone healing. The underlying mechanisms appear to involve active remodeling mediated by the implanted hESC-progenitors maturing into osteoblastic cells and the invading host cells (43).

In summary, we report that perfusion culture is critical for engineering centimeter-size bone grafts from hESC. The engineered bone tissue was stable for 8 wk in vivo and exhibited signs of continued bone development, indicating a potential for bone defect regeneration. Our study shows the possibility to translate the bone tissue engineering protocols developed for adult stem cells (such as those derived from bone marrow aspirates) to embryonic-like stem cells, thereby taking advantage of the potential of pluripotent cell sources for basic and translational studies. The lack of tissue types reminiscent of tumors in engineered bone constructs implanted for 8 wk in vivo suggests at least a short-term stability and safety of engineered bone grafts. Ongoing long-term studies in orthotopic implantation models will help evaluate the safety and functionality of bone grafts engineered from hESC derivatives.

## Methods

Detailed experimental methods are provided as *SI Methods*.

**Cell Culture.** hESC (lines H9 and H13) were induced into mesenchymal lineage in serum-supplemented medium for 7 d, split, and subcultured for up to 55 d (10–11 passages). Expression of surface antigens was determined by flow cytometry. In vitro differentiation potential was evaluated in monolayers and pellet cultures, with BMSC serving as controls.

**Decellularized Bone Scaffolds.** Scaffolds were prepared as in our previous studies (30, 34).

**Perfusion Bioreactor Culture.** hESC-derived progenitors were seeded into scaffolds (1.5 million cells per scaffold) and cultured in osteogenic medium for 3 d to allow cell attachment, and then in either perfusion bioreactors or six-well plates for up to 5 wk (Fig. 1). Medium samples were taken for biochemical assays at each medium change (twice a week). Tissue constructs analyzed after 3 and 5 wk of cultivation (for details, see *SI Methods*).

**Implantation.** Safety and phenotype stability of perfused bone constructs from H9 progenitors were assessed over 8 wk of s.c. implantation in immunodeficient (SCID-beige) mice, according to the Columbia University Institutional Animal Care And Use Committee approved animal protocol. Controls consisted of (*i*) H9-mesenchymal progenitors seeded in scaffolds, (*ii*) undifferentiated H9 cells seeded in scaffolds, and (*iii*) undifferentiated H9 cells encapsulated in Matrigel.

www.manaraa.com

**Statistical Analyses.** Multiway analysis of variance (ANOVA) was followed by Tukey's post hoc analysis by using STATISTICA software, with $P < 0.05$ being considered as statistically significant.

1. Vacanti JP, Langer R (1999) Tissue engineering: The design and fabrication of living replacement devices for surgical reconstruction and transplantation. *Lancet* 354(Suppl 1):SI32–SI34.
2. Scheller EL, Krebsbach PH, Kohn DH (2009) Tissue engineering: State of the art in oral rehabilitation. *J Oral Rehabil* 36:368–389.
3. Hankenson KD, Dishowitz M, Gray C, Schenker M (2011) Angiogenesis in bone regeneration. *Injury* 42:556–561.
4. Marsell R, Einhorn TA (2011) The biology of fracture healing. *Injury* 42:551–555.
5. Muschler GF, Nakamoto C, Griffith LG (2004) Engineering principles of clinical cell-based tissue engineering. *J Bone Joint Surg Am* 86-A:1541–1558.
6. Grayson WL, Chao PH, Marolt D, Kaplan DL, Vunjak-Novakovic G (2008) Engineering custom-designed osteochondral tissue grafts. *Trends Biotechnol* 26:181–189.
7. Vunjak-Novakovic G, Meinel L, Altman G, Kaplan D (2005) Bioreactor cultivation of osteochondral grafts. *Orthod Craniofac Res* 8:209–218.
8. Marolt D, Knezevic M, Novakovic GV (2010) Bone tissue engineering with human stem cells. *Stem Cell Res Ther* 1:10.
9. Vunjak-Novakovic G, Scadden DT (2011) Biomimetic platforms for human stem cell research. *Cell Stem Cell* 8:252–261.
10. Zaidi M (2007) Skeletal remodeling in health and disease. *Nat Med* 13:791–801.
11. Thomson JA, et al. (1998) Embryonic stem cell lines derived from human blastocysts. *Science* 282:1145–1147.
12. Barberi T, Willis LM, Socci ND, Studer L (2005) Derivation of multipotent mesenchymal precursors from human embryonic stem cells. *PLoS Med* 2:e161.
13. de Peppo GM, et al. (2010) Human embryonic mesodermal progenitors highly resemble human mesenchymal stem cells and display high potential for tissue engineering applications. *Tissue Eng Part A* 16:2161–2182.
14. Lian Q, et al. (2007) Derivation of clinically compliant MSCs from CD105+, CD24-differentiated human ESCs. *Stem Cells* 25:425–436.
15. Olivier EN, Rybicki AC, Bouhassira EE (2006) Differentiation of human embryonic stem cells into bipotent mesenchymal stem cells. *Stem Cells* 24:1914–1922.
16. Ahn SE, et al. (2006) Primary bone-derived cells induce osteogenic differentiation without exogenous factors in human embryonic stem cells. *Biochem Biophys Res Commun* 340:403–408.
17. Kuznetsov SA, Cherman N, Robey PG (2011) In vivo bone formation by progeny of human embryonic stem cells. *Stem Cells Dev* 20:269–287.
18. Mateizel I, et al. (2008) Efficient differentiation of human embryonic stem cells into a homogeneous population of osteoprogenitor-like cells. *Reprod Biomed Online* 16:741–753.
19. Hwang NS, et al. (2008) In vivo commitment and functional tissue regeneration using human embryonic stem cell-derived mesenchymal cells. *Proc Natl Acad Sci USA* 105:20641–20646.
20. Oldershaw RA, et al. (2010) Directed differentiation of human embryonic stem cells toward chondrocytes. *Nat Biotechnol* 28:1187–1194.
21. James D, et al. (2010) Expansion and maintenance of human embryonic stem cell-derived endothelial cells by TGFbeta inhibition is Id1 dependent. *Nat Biotechnol* 28:161–166.
22. Yang L, et al. (2008) Human cardiovascular progenitor cells develop from a KDR+ embryonic-stem-cell-derived population. *Nature* 453:524–528.
23. Lee H, et al. (2007) Directed differentiation and transplantation of human embryonic stem cell-derived motoneurons. *Stem Cells* 25:1931–1939.
24. Bock C, et al. (2011) Reference Maps of human ES and iPS cell variation enable high-throughput characterization of pluripotent cell lines. *Cell* 144:439–452.
25. Takahashi K, et al. (2007) Induction of pluripotent stem cells from adult human fibroblasts by defined factors. *Cell* 131:861–872.
26. Warren L, et al. (2010) Highly efficient reprogramming to pluripotency and directed differentiation of human cells with synthetic modified mRNA. *Cell Stem Cell* 7:618–630.
27. Bielby RC, Boccaccini AR, Polak JM, Buttery LD (2004) In vitro differentiation and in vivo mineralization of osteogenic cells derived from human embryonic stem cells. *Tissue Eng* 10:1518–1525.
28. Kim S, et al. (2008) In vivo bone formation from human embryonic stem cell-derived osteogenic cells in poly(d,l-lactic-co-glycolic acid)/hydroxyapatite composite scaffolds. *Biomaterials* 29:1043–1053.
29. Olsen BR, Reginato AM, Wang W (2000) Bone development. *Annu Rev Cell Dev Biol* 16:191–220.
30. Grayson WL, et al. (2011) Optimizing the medium perfusion rate in bone tissue engineering bioreactors. *Biotechnol Bioeng* 108:1159–1170.
31. Pittenger MF, et al. (1999) Multilineage potential of adult human mesenchymal stem cells. *Science* 284:143–147.
32. Jaiswal N, Haynesworth SE, Caplan AI, Bruder SP (1997) Osteogenic differentiation of purified, culture-expanded human mesenchymal stem cells in vitro. *J Cell Biochem* 64:295–312.
33. de Peppo GM, et al. (2010) Osteogenic potential of human mesenchymal stem cells and human embryonic stem cell-derived mesodermal progenitors: A tissue engineering perspective. *Tissue Eng Part A* 16:3413–3426.
34. Grayson WL, et al. (2008) Effects of initial seeding density and fluid perfusion rate on formation of tissue-engineered bone. *Tissue Eng Part A* 14:1809–1820.
35. Grayson WL, et al. (2010) Engineering anatomically shaped human bone grafts. *Proc Natl Acad Sci USA* 107:3299–3304.
36. Holtorf HL, Jansen JA, Mikos AG (2005) Flow perfusion culture induces the osteoblastic differentiation of marrow stroma cell-scaffold constructs in the absence of dexamethasone. *J Biomed Mater Res A* 72:326–334.
37. Sikavitsas VI, Bancroft GN, Holtorf HL, Jansen JA, Mikos AG (2003) Mineralized matrix deposition by marrow stromal osteoblasts in 3D perfusion culture increases with increasing fluid shear forces. *Proc Natl Acad Sci USA* 100:14683–14688.
38. Zeng Y, Cowin SC, Weinbaum S (1994) A fiber matrix model for fluid flow and streaming potentials in the canaliculi of an osteon. *Ann Biomed Eng* 22:280–292.
39. Grayson WL, Bhumiratana S, Grace Chao PH, Hung CT, Vunjak-Novakovic G (2010) Spatial regulation of human mesenchymal stem cell differentiation in engineered osteochondral constructs: Effects of pre-differentiation, soluble factors and medium perfusion. *Osteoarthritis Cartilage* 18:714–723.
40. Bhumiratana S, et al. (2011) Nucleation and growth of mineralized bone matrix on silk-hydroxyapatite composite scaffolds. *Biomaterials* 32:2812–2820.
41. Gruenloh W, et al. (2011) Characterization and in vivo testing of mesenchymal stem cells derived from human embryonic stem cells. *Tissue Eng Part A* 17:1517–1525.
42. Oest ME, Dupont KM, Kong HJ, Mooney DJ, Guldberg RE (2007) Quantitative assessment of scaffold and growth factor-mediated repair of critically sized bone defects. *J Orthop Res* 25:941–950.
43. Tang Y, et al. (2009) TGF-beta1-induced migration of bone mesenchymal stem cells couples bone resorption with formation. *Nat Med* 15:757–765.

MEDICAL SCIENCES

Marolt et al.

www.manaraa.com